Doxorubicin encapsulated hollow self-assembled CuS nanoparticles clusters for bio-responsive chemo-photo therapy

Chakraborty, Swaroop; Prasad, Rajendra; Pandey, Pramina Kumari; Khan, Amreen; Jain, Nishant Kumar; Jones, Eugenia Valsami; Srivastava, Rohit; Misra, Superb K.

DOI:
10.1016/j.matlet.2022.133017

Materials Letters 327 (2022) 133017

Contents lists available at ScienceDirect

Materials Letters

journal homepage: www.elsevier.com/locate/matlet

Doxorubicin encapsulated hollow self-assembled CuS nanoparticles clusters for bio-responsive chemo-photo therapy

Swaroop Chakraborty [a,c,*,1], Rajendra Prasad [b,1], Pramina Kumari Pandey [c,1], Amreen Khan [b,d], Nishant Kumar Jain [b], Eugenia Valsami Jones [a], Rohit Srivastava [b], Superb K. Misra [c,*]

[a] Geography, Earth and Environmental Sciences, University of Birmingham, B152TT, UK
[b] Biosciences and Bioengineering, IIT Bombay, 400076, India
[c] Materials Engineering, Indian Institute of Technology Gandhinagar, 382355, India
[d] Center for Research in Nanotechnology & Science, IIT Bombay, 400076, India

ARTICLE INFO

Keywords:
Photothermal therapy
CuS nanoparticles
Self-assembled clusters
Chemotherapy
Doxorubicin

ABSTRACT

Herein, we reported self-assembled highly dispersed hollow CuS nanoparticle clusters (CuS NC) with promising photothermal efficiency of 40.5 %, uniform particle size distribution (~150 nm), porosity and exhibiting high biocompatibility. Further, these designed photothermal hybrid structures are engineered with Doxorubicin anticancer drug molecules (DOX@CuS NC) for bio-responsive chemo-photo therapy of breast cancer (>70 % cell death at a concentration of 20 μg mL^{-1}).

1. Introduction

Recently, combinatorial therapies viz., chemo-photothermal, chemo-photodynamic, chemo-radiation, photothermal-photodynamic, and chemo-sonodynamic have shown a significant improvement over standalone cancer therapeutics approach [1,2]. The combinatorial approach has the advantage of minimal invasion, use of low drug concentration, site-selectivity, image-guided therapeutics ability, and synergistic anticancer activity [3]. To the best of our knowledge, several nanohybrids have been proposed for combination therapy of cancer, however, low therapeutics response and uncontrolled particle size distribution with poor drug loading are major limitations [1]. In addition, low photostability, reduced NIR absorption after the repetitive laser irradiation, and poor intracellular accumulation are major limitations of these nanostructures [1,2,4]. Therefore, there is a need of designing a novel multifunctional nanocarrier with a high bio-responsive, biocompatibility, easy and cost-effective synthesis process, high surface area and higher photothermal conversion efficiency. In our study (Fig. 1), we synthesized novel CuS nanoparticle clusters (CuS NC) with good hydrodynamic stability, high photothermal conversion efficiency and biocompatibility. To have a combinatorial effect, the hollow CuS NC were loaded with Doxorubicin (DOX), wherein the porosity aided the impregnation of DOX into the CuS NC structure and contributed toward combined chemo-photothermal therapy.

2. Experimental section

Hollow CuS NC were synthesized via sulfidation reaction at 60 °C by using Cu_2O spheres as a sacrificial template. Briefly, 0.48 g of polyvinylpyrrolidone was dissolved in 50 mL of ultra-pure water followed by dropwise addition of 200 μL of $CuCl_2{\cdot}2H_2O$ (0.5 M) solution. The solution was stirred at 750 rpm at 25 °C. Subsequently, 50 mL NaOH (pH 10.8) was added, followed by the addition of hydrazine hydrate (15 μL) solution to form Cu_2O nanospheres. After 5 min stirring, the suspension was heated to 60 °C and 400 μL Na_2S solution (180 $mgmL^{-1}$) was added dropwise under stirring conditions for 3.5 hrs. The hollow CuS NC were collected by centrifugation (13500 rpm, 30 min) and washed twice with ultra-pure water. The pellet was redispersed in ultrapure water and stored for further use. The detailed experimental characterization, DOX loading and release; biological studies are discussed in the supplementary information file (SI). The hollow interior of CuS NC encircling a porous shell formed by small CuS nanocrystals (~10.8 ± 2 nm) due to the Kirkendall effect was confirmed through transmission electron microscopy (TEM, Themis-300, Thermofisher Scientific) [3,5]. Time-dependent hydrodynamic stability studies (Zetasizer Nano ZS, Malvern, UK) were performed for CuS NC in several biological relevant

* Corresponding author at: Geography, Earth and Environmental Sciences, University of Birmingham, B152TT, UK (S. Chakraborty).
E-mail addresses: s.chakraborty@bham.ac.uk (S. Chakraborty), smisra@iitgn.ac.in (S.K. Misra).
[1] Authors contributed equally.

https://doi.org/10.1016/j.matlet.2022.133017
Received 7 February 2022; Received in revised form 10 August 2022; Accepted 14 August 2022
Available online 17 August 2022

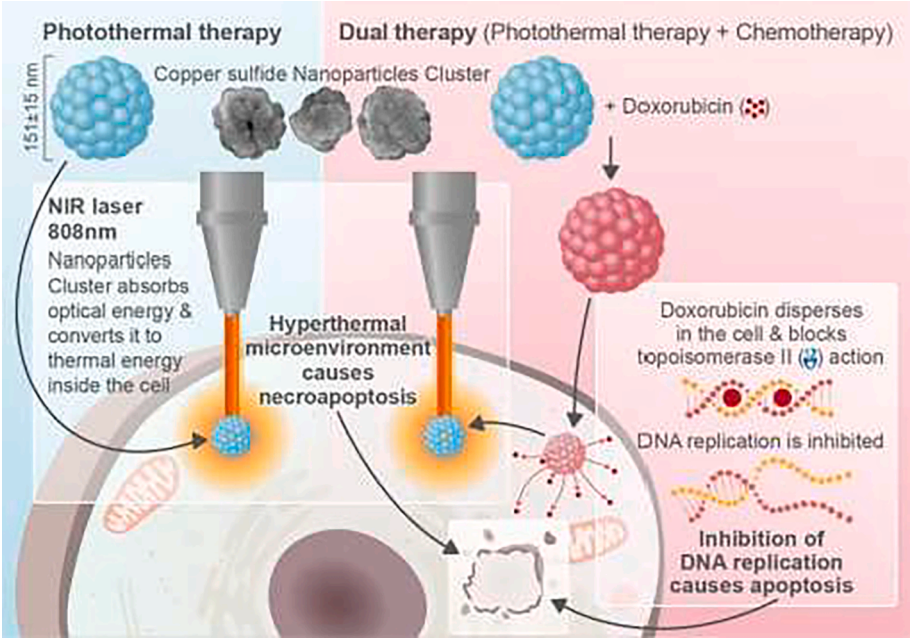

Fig. 1. Schematic demonstrating the efficacy of using DOX loaded CuS nanoparticle clusters (DOX@CuS NC) as a dual therapy agent (photothermal and chemotherapy) against MCF7 cells.

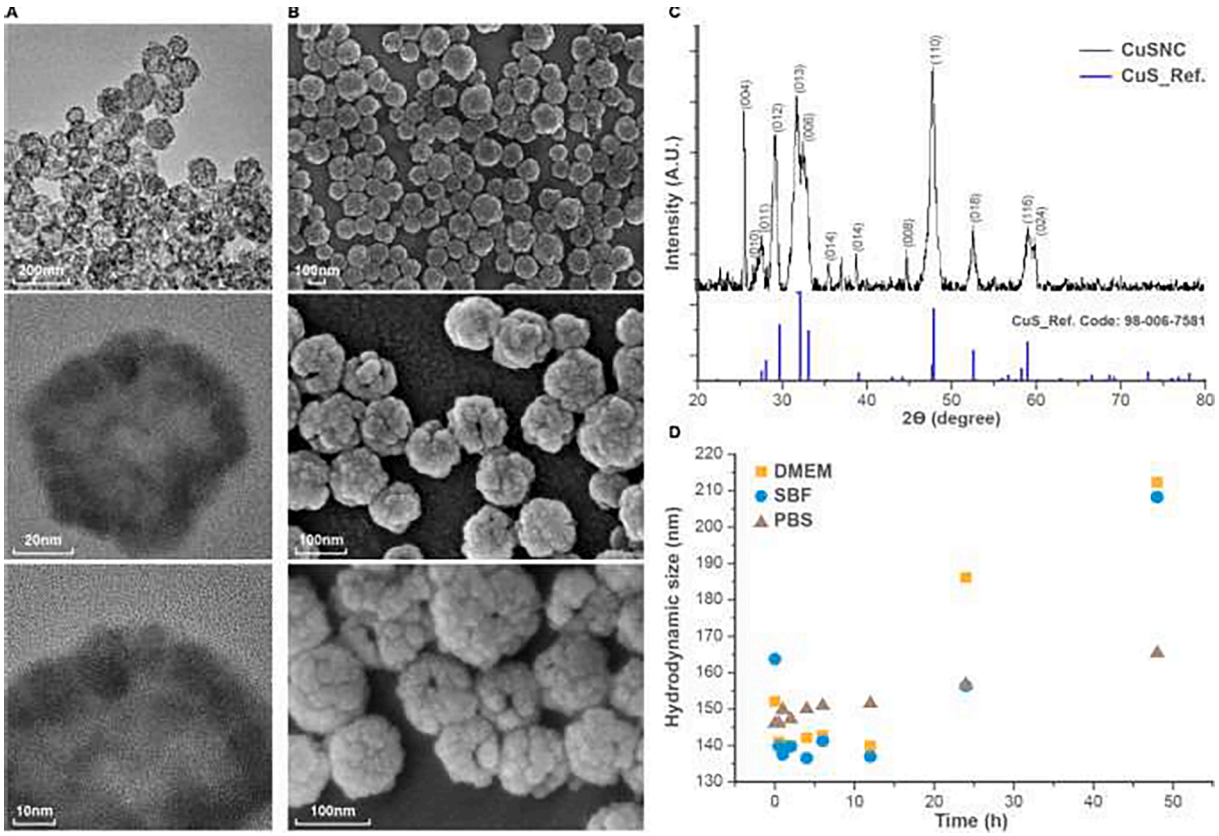

Fig. 2. Characterization of porous CuS NC showing the (A-B) TEM and SEM images, with the average nanoparticle cluster size measured as 150 ± 15 nm. Each of these nanoclusters is composed of CuS nanoparticles whose size is 10.8 ± 2 nm. (C) XRD pattern of CuS NC showing the phase purity of the particles. (D) Variation in hydrodynamic size of CuS NC in three different simulated biological media i.e., DMEM, SBF and PBS for 48 hrs.

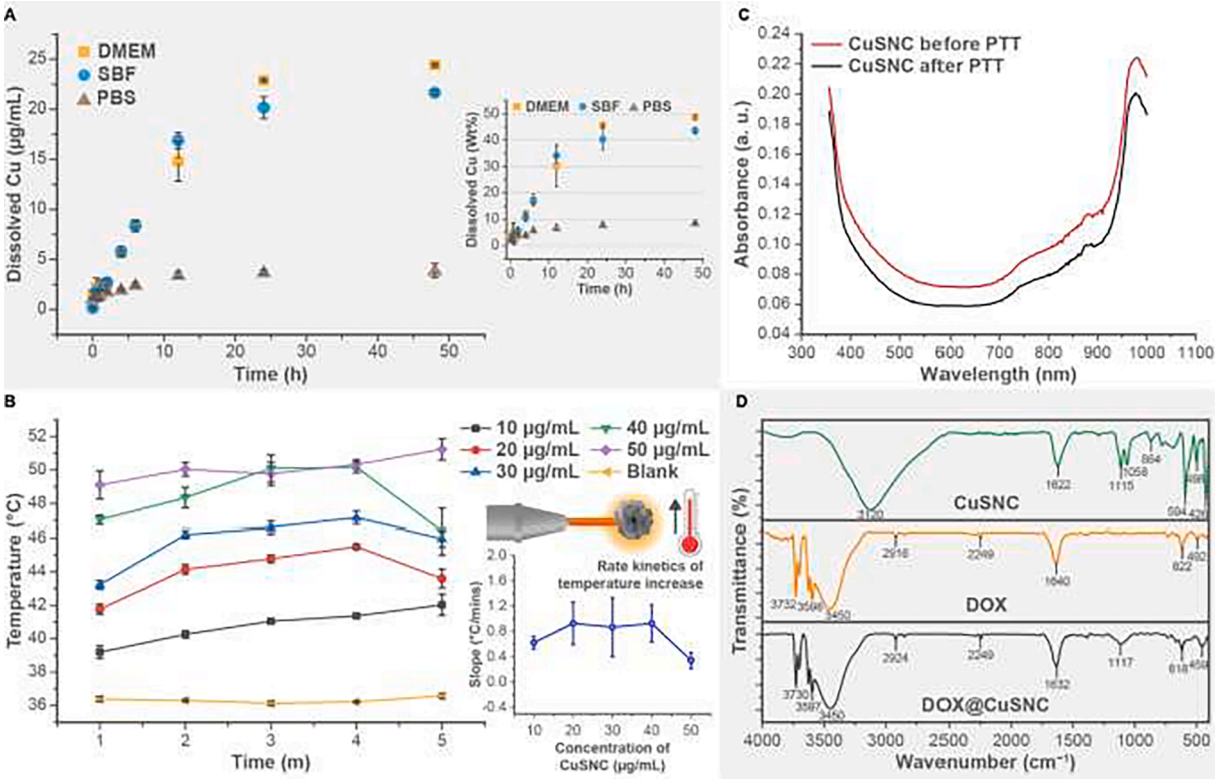

Fig. 3. (A) Dissolution profile of CuS NC in PBS, SBF and DMEM at a concentration of 50 μg mL^{-1}, (B) Photothermal response of CuS NC after NIR laser irradiation (1.0 W cm^{-2}) at different time intervals and concentration, and the rate kinetics of temperature rise. (C) UV–Vis spectra of CuS NC before and after laser irradiation, (D) FTIR spectra demonstrating the loading of DOX on the CuS NC.

media (DMEM cell culture medium, simulated body fluid and phosphate buffer saline) at 37 °C.

3. Results and discussion

3.1. Characterization studies

As shown in Fig. 2A and Fig. 2B, the CuS NC showed a mean size of

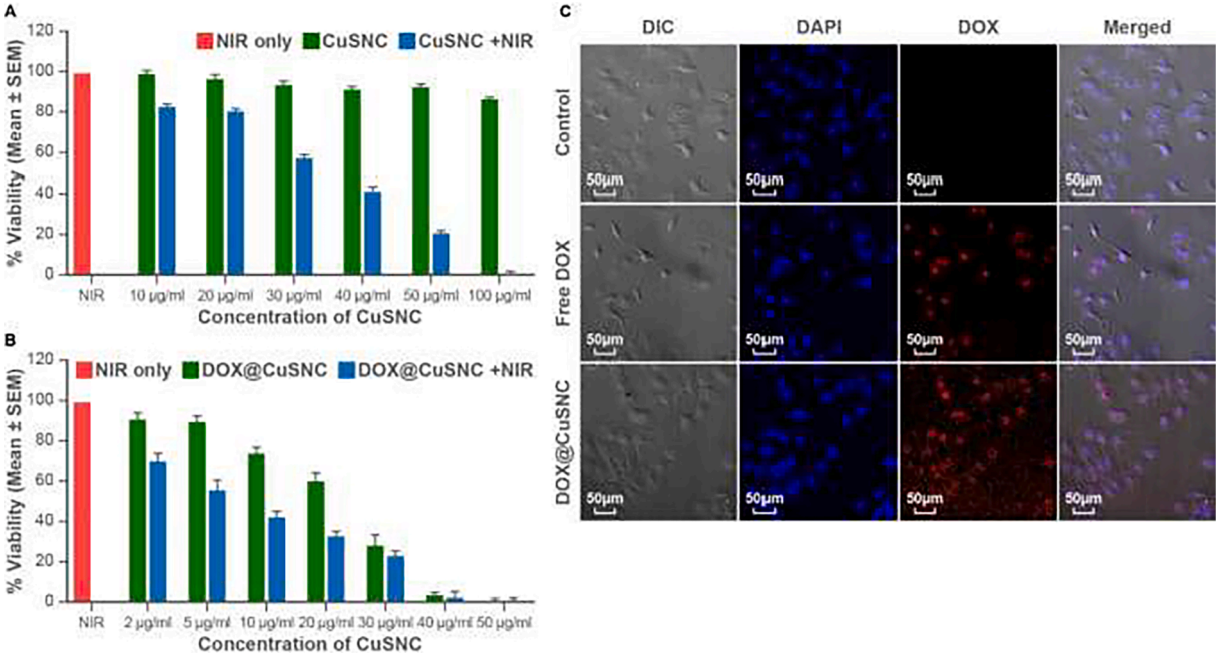

Fig. 4. Cytotoxicity profile of MCF-7 cells on exposure to standalone CuS NC (A-B) and DOX@CuS NC with 808 nm NIR laser irradiation having a power density of 1.0 W cm^{-2} for 5 min. (C) Cellular uptake of free DOX and DOX@CuS NC with a clear distinction in higher cellular uptake of DOX@CuS NC. (Red: Doxorubicin, Blue: DAPI stain). (For interpretation of the references to colour in this figure legend, the reader is referred to the web version of this article.)

150 ± 15 nm and were uniformly distributed with spherical morphology and a porous structure. These CuS NC are highly aggregated structures made of small CuS nanocrystals of size 10.8 ± 2 nm (measured by using ImageJ software) that make the clusters highly porous for better drug loading, minimising the drug leakage, and improving the loading efficiency of nanocarriers. The hollow mesoporous CuS NC showed a BET surface area of 25.4 $m^2 g^{-1}$ with a pore size of 9.1 nm. CuS nanoparticle clusters were confirmed by XRD analysis (Rigaku LX-578; Cu-Kα λ = 1.5418 Å, Fig. 2C). The hydrodynamic size of CuS NC increased from 140 nm to 215 nm in DMEM media: 140 nm to 210 nm in SBF, and from 145 nm to 160 nm in PBS at the end of 48 h (Fig. 2D). The zeta potential of the nanoparticle cluster suspension in deionized water was −14.5 ± 1.43 mV indicating their aqueous stability.

Fig. 3A shows the dissolution behaviour of CuS NC in DMEM, SBF and PBS. The solubility experiments were conducted using a dialysis membrane-based technique (MWCO = 3.5 kDa) [6]. For CuS NC concentration of 67 μg mL^{-1} (Cu concentration = 50 μg mL^{-1}) at the end of 48 h, ~50 wt% dissolved Cu was present in DMEM, ~42 wt% dissolved Cu was present in SBF and < 7 % dissolved Cu were present in PBS. The rate of dissolution (calculated by using a modified first-order exponential rate equation) of CuS NC in DMEM, SBF and PBS was found to be −0.08 h^{-1}, −0.05 h^{-1} and −0.1 h^{-1}, respectively. The process of dissolution is very critical in dictating the cellular response of CuS NC. For example, copper-based nanomaterials have shown some toxicity to mammalian cells at a higher exposure concentration due to depletion of glutathione, lipid peroxidation, and superoxide dismutase induction [6–8].

Engineered CuS NC absorb NIR light at 808 nm and produces a clear photothermal-based temperature rise at the rate of ~0.86 °C min^{-1}. In the control sample (ultrapure water), exposure to NIR light did not result in any rise in temperature beyond 37 °C. In comparison, a 5 min exposure to NIR light resulted in a significant temperature rise across all concentrations of CuS NC. The photothermal efficiency (η) was found to be 40.5 % (detailed calculation in SI), which makes the hollow CuS NC a promising material for efficient photothermal therapy. The CuS NC were observed to be photostable post-irradiation (Fig. 3C). FTIR spectra (Fig. 3D) show the presence of characteristic peaks of DOX in CuS NC i.e., 3730 cm^{-1}, 3597 cm^{-1}, 3450 cm^{-1}, 2924 cm^{-1} and 2249 cm^{-1}, representing the OH stretching, phenol groups, bond stretching of amine group, C—H group, C—N group. The spectra clearly show that after 24 hrs of incubation, DOX is adsorbed in the porous structure of CuS NC. The concentration of DOX was estimated to be 63 ± 2.4 μg mg^{-1} of CuS NC, which corresponds to a DOX loading of 63 %. The DOX loading on CuS NC was about 63 % and release profile has been shown in SI (Figure S6).

3.2. Chemo-photothermal properties

CuS NC was observed to be cytocompatible on L929 fibroblast cell lines with an insignificant loss in cell viability (Figure S1 and S4). The PTT efficiency on breast cancer cell line MCF7 cells was observed to be irradiation time and concentration-dependent (Fig. 4A). The cell viability decreased further when the concentration of CuS NC increases from 30 μg mL^{-1} to 40 μg mL^{-1}. While CuS NC can be tolerated by the cells for up to 100 μg mL^{-1}, in the presence of NIR, the PTT effect kicks in and particle concentration >30 μg mL^{-1} becomes toxic to the cells. Therefore, the developed hollow CuS NC can balance between cytotoxicity and photothermal effect to regulate the therapeutic efficacy.

The toxicity towards MCF-7 cells was further enhanced when DOX@CuS NC was irradiated with a NIR laser for 5 min. The reduction in cell viability for 30 μg mL^{-1} CuS NC and DOX@CuS NC was observed to be 42 ± 0.8 % and 77 ± 1.8 % respectively. There was an enhancement of 25 % in cytotoxicity with co-application of DOX-based chemotherapy and PTT. Literature shows that the DOX@CuS NC is endocytosed by the cells, prolongs the residence time, and enhances the content that allows a sustained diffusion of DOX inside the cells [9]. Fig. 4B confirms that compared to CuS NC, DOX@CuS NC has a stronger cytotoxic efficiency against the MCF-7 cells after the irradiation. The encouraging results indicate that DOX@CuS NC based chemo-PTT system is highly efficient as compared to that of standalone PTT or chemotherapy. The rise in temperature within the cellular microenvironment is enhancing the process of DOX diffusion in the cell and therefore causing a synergistic effect of chemo-PTT therapy. To prove this, we investigated the cellular uptake of DOX when delivered as DOX@CuS NC as compared to free DOX in MCF-7 cells after 24 hrs. Fig. 4C illustrates the intracellular accumulation of free DOX and DOX@CuS NC in MCF-7 cells using confocal microscopy. The distribution of free DOX in MCF-7 cells was found to be lower compared to DOX@CuS NC. The free DOX is delivered inside the cells mainly by the process of diffusion. The major factor determining the anti-cancer potency of any chemotherapeutic drug is its intracellular drug bioavailability, accumulation, and active metabolism in the targeted system [1,2]. The mechanism of action of DOX has been established in sufficient detail. The intercalation of DOX molecules with DNA causes alteration in gene expression, followed by the production of ROS and inhibiting the action of enzyme topoisomerase to stop DNA synthesis [10].

4. Conclusions

In summary, we synthesized highly porous and hollow CuS NC (~150 nm) by the process of self-assembly of small CuS nanocrystals (~10 nm). Upon NIR light exposure (808 nm), Doxorubicin loaded CuS NC exhibits a photothermal efficiency of 40.5 % and the photothermal temperature rise was ~0.86 °C min^{-1}. The synthesized CuS NC showed promising biocompatibility with L929 fibroblast cells. DOX@CuS NC showed significant cell cytotoxicity to MCF7 breast cancer cells with NIR treatment wherein there was >60 % reduction in cell viability with exposure concentration as low as 10 μgmL^{-1}. Overall, the engineered hollow CuS NC could be considered a safe biomaterial for drug delivery and combined chemo-phototherapy of cancer.

Declaration of Competing Interest

The authors declare that they have no known competing financial interests or personal relationships that could have appeared to influence the work reported in this paper.

Acknowledgment

This work has been financially supported by IMPRINT (Project No. 6408, MHRD), and SERB-CRG (CRG/2019/006165). he authors would like to acknowledge the equipment support provided by DST-FIST through SR/FST/ET-I/2017/18.

Appendix A. Supplementary data

Supplementary data to this article can be found online at https://doi.org/10.1016/j.matlet.2022.133017.

References

[1] R. Prasad, D.S. Chauhan, A.S. Yadav, et al., Nanoscale (2018) 19082–19091.
[2] D.S. Chauhan, R. Prasad, J. Devrukhkar, et al., Bioconjug. Chem. (2018) 1510–1518.
[3] S. Nilsson, D. Albinsson, T.J. Antosiewicz, et al., Nanoscale (2019) 20725–20733.
[4] X. Liu, B. Li, F. Fu, et al., Dalton Trans. (2014) 11709–11715.
[5] K. Liu, J.J. Zhang, F.F. Cheng, et al., J. Mater. Chem. (2011) 12034–12040.
[6] S. Chakraborty, A. Nair, M. Paliwal, et al., J. Nanopart. Res. (2018) 1–14.
[7] S. Chakraborty, S.K. Misra, Environ. Nanotechnol., Monitor. Manage. (2019) 100258.
[8] C. Angelé-Martínez, K.V.T. Nguyen, F.S. Ameer, et al., Nanotoxicology (2017) 278–288.
[9] H. Bi, Y. Dai, R. Lv, C. Zhong, et al., Dalton Trans. (2016) 5101–5110.
[10] F. Yang, S.S. Teves, C.J. Kemp, et al., Biochim. Biophys. Acta (BBA)-Rev. Cancer (2014,) 84–89.